ADVANCED
ELECTRONIC
MATERIALS

Supporting Information

for *Adv. Electron. Mater.*, DOI: 10.1002/aelm.202001023

Self-Healing Thin-Film Transistor Circuits on Flexible Substrates

*Li Ding, Pushkaraj Joshi, James Macdonald, Virendra Parab, and Sanjiv Sambandan**

Supporting Information

Self-Healing Thin Film Transistor Circuits on Flexible Substrates

*Li Ding, Pushkaraj Joshi, James Macdonald, Virendra Parab and Sanjiv Sambandan**

Li Ding, Dr. Pushkaraj Joshi, Prof. Sanjiv Sambandan
Nanoscience Centre, Department of Engineering, University of Cambridge, 11 JJ Thomson Ave, Cambridge CB30FF, UK
E-mail: ss698@cam.ac.uk

James Macdonald
Institute for Manufacturing, Department of Engineering, University of Cambridge, 17 Charles Babbage Road, Cambridge CB30FS, UK

Virendra Parab, Prof. Sanjiv Sambandan
Department of Instrumentation and Applied Physics, Indian Institute of Science, Bangalore, 560012, India
E-mail: sanjiv@iisc.ac.in

Text S1: Optimization of dispersion concentration

We decide the optimum dispersion concentration for Ag particles based on the prior calculated optimum concentration for Cu particles.[34] We define the optimum dispersion of copper and silver particles in silicon oil in weight/volume as ϕ_{Cu} and ϕ_{Ag}, respectively. We assume that the dispersion has a 2D spread. This implies the distance between 2 particles scales as $n^{-1/2}$ where n is numbers of particles per unit volume. If r_{Cu} is the radius of the Cu particle, ρ_{Cu} the mass density of Cu particle, r_{Ag} the radius of Ag particle and ρ_{Ag} the mass density of Ag particle, $n_{Cu} = \phi_{Cu}/(4/3\pi r_{Cu}^3 \rho_{Cu})$ and $n_{Ag} = \phi_{Ag}/(4/3\pi r_{Ag}^3 \rho_{Ag})$. The distance between two Cu particles and two Ag particles in their respective 2D flattened dispersions are, $x_{Cu} \cong n_{Cu}^{-1/2} = (\frac{\phi_{Cu}}{4/3\pi r_{Cu}^3 \rho_{Cu}})^{-1/2}$ and $x_{Ag} \cong n_{Ag}^{-1/2} = (\frac{\phi_{Ag}}{4/3\pi r_{Ag}^3 \rho_{Ag}})^{-1/2}$, respectively. To identify ϕ_{Ag} from our knowledge of ϕ_{Cu}, we aim to keep the heal time constant i.e.

$\tau_{h,Cu} \propto \left(\frac{x_{Cu}}{r_{Cu}}\right)^5 = \tau_{h,Ag} \propto (\frac{x_{Ag}}{r_{Ag}})^5$. We therefore need $\frac{x_{Cu}}{r_{Cu}} = \frac{x_{Ag}}{r_{Ag}}$ => $\frac{\phi_{Cu}^{-1/2}}{r_{Cu}^{-1/2}\rho_{Cu}^{-1/2}} = \frac{\phi_{Ag}^{-1/2}}{r_{Ag}^{-1/2}\rho_{Ag}^{-1/2}}$.

Therefore, $\phi_{Ag} = \phi_{Cu}(\frac{r_{Ag}}{r_{Cu}})(\frac{\rho_{Ag}}{\rho_{Cu}})$.

$\phi_{Cu} \cong 150$ mg/ml. Therefore, $\phi_{Ag} \cong 150 \times (\frac{0.5}{5})(\frac{10.49}{8.9}) \approx 17.68$ mg/ml

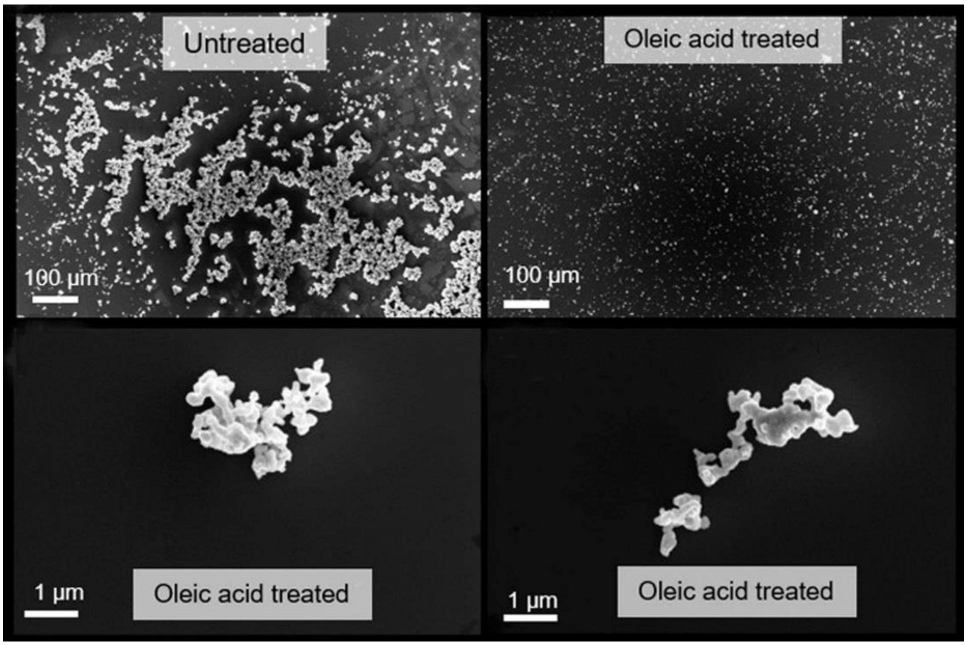

Figure S1: Effect of oleic acid treatment on aggregation of particles. FESEM images of untreated and oleic acid treated silver powder along with their magnified view. The samples are prepared by suspending the powders in hexane and drop-cast on silicon wafer.

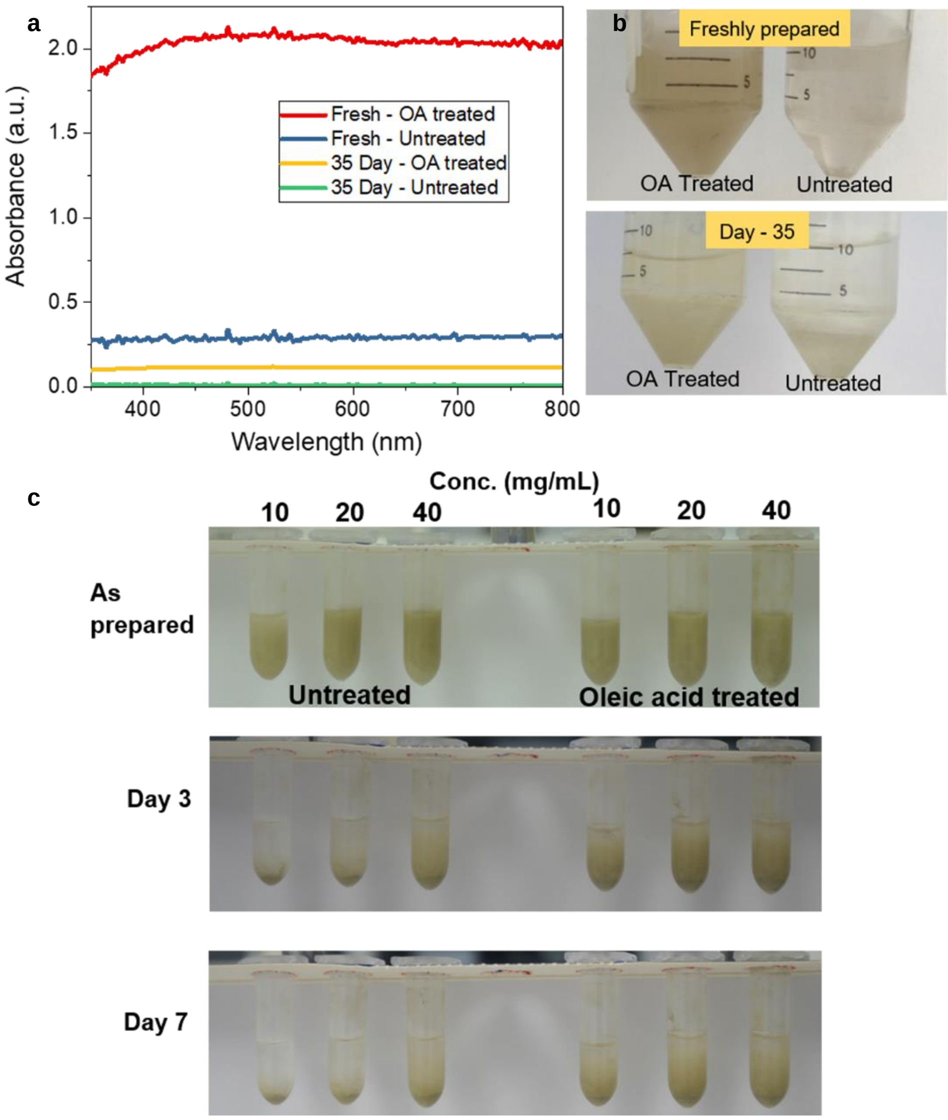

Figure S2: Effect of oleic acid treatment on stability of suspension. (a). UV-Visible absorbance of the suspension freshly prepared and after 35 days of settling. (b). Photograph of freshly prepared dispersion of untreated and oleic acid treated silver powder suspended in silicone oil (1 mg/mL) and after 35 days of settling. (c). Photographs illustrating the settling behaviour of uncapped and oleic acid capped silver powder suspended in silicone oil with varying concentrations of 10, 20 and 40 mg/mL observed on day 0, day 3 and day 7.

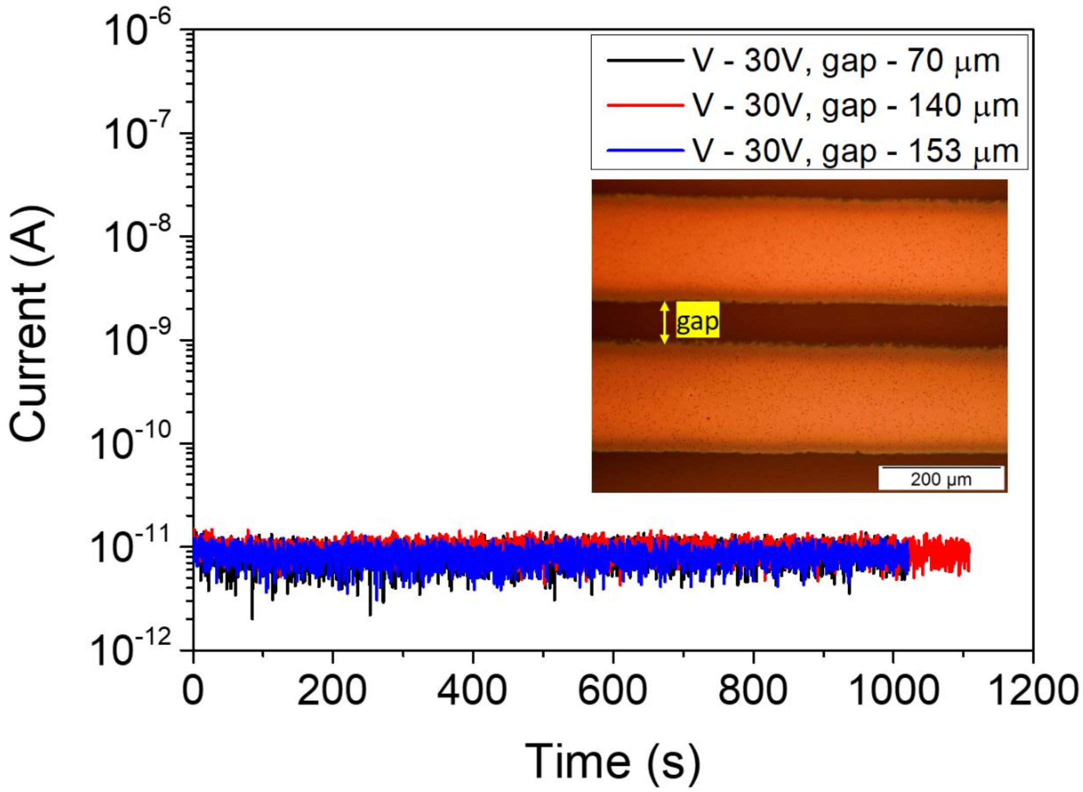

Figure S3. Inherently insulating nature of the dispersion. The insulating nature of the dispersion of 20 mg/mL silver particles is demonstrated by pouring the dispersion across interconnects (inset) with different gap size (70, 140 and 153 μm) and monitoring the current across them under applied voltage of 30V.

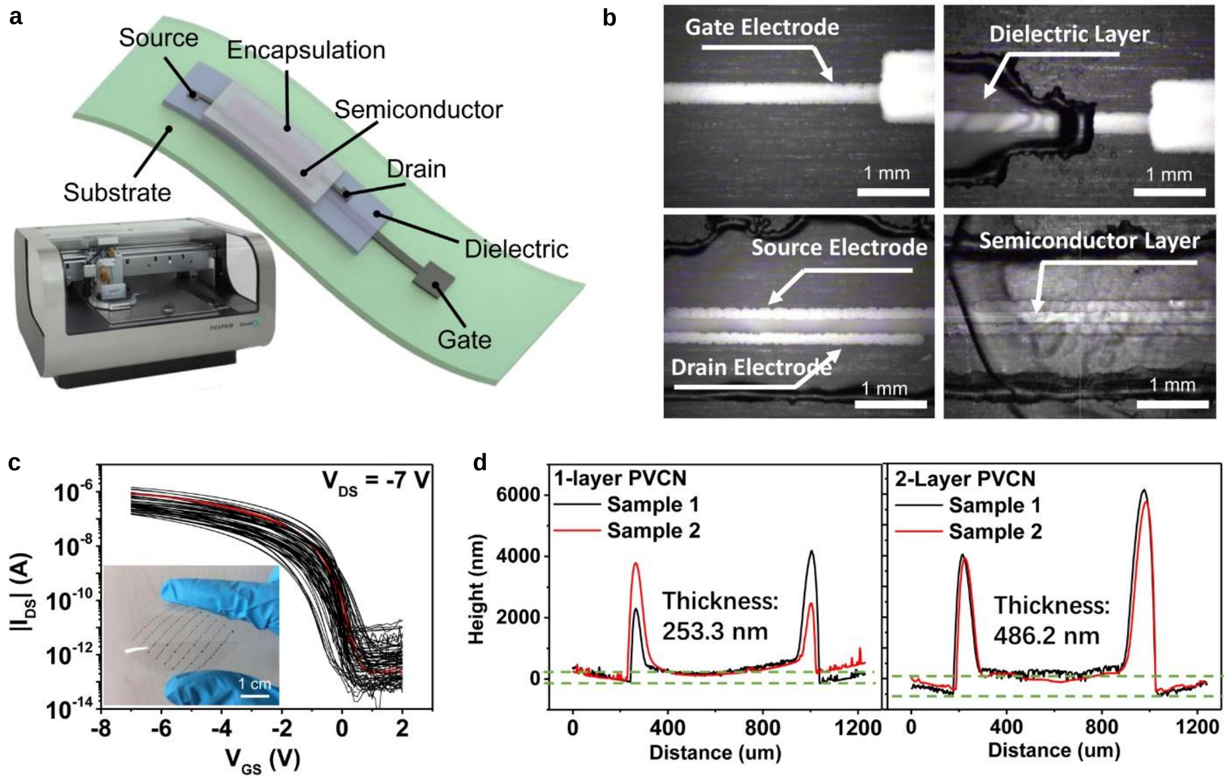

Figure S4. Inkjet fabrication and characterization of thin film transistor. (a) Schematic of OTFT device showing the bottom-gate bottom-contact (BGBC) device structure, and photograph of the ink-jet printer Fujifilm Dimatix DMP-2831. (b) Photographs illustrating the inkjet patterning of gate electrode, dielectric layer, source / drain electrodes and semiconducting layer during the fabrication of BGBC configuration of OTFT. (c) Transfer characteristics plotted as I_{DS} versus V_{GS} of 47 inkjet-printed OTFT devices used in this study. The red trace indicates the typical transfer curve as shown in **Figure 1c.** The inset shows a photograph of an array of OTFT devices patterned on PEN substrate. (d) Dektak profilometer trace of 1-layer and 2-layer dielectric film for thickness measurement measured over 2 samples.